

# Green synthesis of nanoporous Si/C anode using NaCl template with improved cycle life

Xu Fan<sup>a,b</sup>, Xiangping Jiang<sup>a,\*</sup>, Wei Wang<sup>b,\*</sup>, Zhaoping Liu<sup>b,\*</sup>

<sup>a</sup> Department of Material Science and Engineering, Jiangxi Key Laboratory of Advanced Ceramic Materials, Jingdezhen Ceramic Institute, Jingdezhen 333001, Jiangxi, China

<sup>b</sup> Ningbo Institute of Materials Technology & Engineering (NIMTE), Chinese Academy of Sciences, Ningbo, Zhejiang 315201, China

---

## ARTICLE INFO

**Keywords:**  
Nanocomposites  
Porous materials  
Silicon anodes  
Green synthesis  
Environment-friendly

---

## ABSTRACT

Porous silicon/carbon (Si/C) structure has been proved of great help to enhance the electrochemical cycling performance of Si-based anode materials. Current fabrication of porous Si based anodes usually relies on the complicated chemical etching process with unavoidable pollution problem. Herein, a nanoporous Si/C composite was successfully fabricated by a facile spray drying and carbonization process. The environmentally benign NaCl is used as the sacrificing template for the generation of embedded nanopores, which can be easily removed by routine washing process. The as-prepared nanoporous Si/C anode exhibits a high reversible specific capacity of around  $900 \text{ mAh g}^{-1}$  with 78.2% capacity retention after 100 cycles. This synthetic method paves a simple and environment-friendly way to build porous Si based anode with improved electrochemical performance which is significantly important for the industrial production.

---

## 1. Introduction

Silicon (Si) is an exciting and promising anode material to replace conventional graphite for the next generation Li-ion battery applications due to its highest theoretical capacity of  $3579 \text{ mA h g}^{-1}$  [1–3]. However, silicon anodes suffers from large volume changes over 300% during the lithiation/delithiation processes, which leads to rapid capacity fading due to pulverization of Si, unstable solid-electrolyte-interphase formation, and contact loss between active particles and conducting agents [4,5].

To address these problems, besides the early works using inactive materials and nanomaterials [6–11], porous architecture is becoming the most effective way to improve the cycle life because the nanopores embedded can accommodate the volume expansion to stabilize the electrode structure. Currently, various porous Si structures have been successfully fabricated by etching, reduction of porous silica and some specific chemical reactions [12–15]. However, these methods are not suitable for the practical applications due to their complicated and high cost synthesis process. More recently, pioneered by Cui et al. [16], another effective way to accommodate the volume expansion is to engineer pores inside the Si based electrode by removing the sacrificing particles

embedded in the fabrication process. In previous work in our group, porous Si/C composites have been successfully fabricated by etching away the sacrificing  $\text{SiO}_2$  nanoparticles, which finally reveal a high capacity of around  $800 \text{ mAh g}^{-1}$  for over 200 cycles [17]. However, in most works related to porous Si based electrodes,  $\text{SiO}_2$  is widely used as the skeleton or sacrificing material, and has to be removed by HF solution considering the dissolution of Si in alkaline solution. It is known that HF is quite harmful and has to be carefully handled, which greatly influence the application of porous Si electrodes in practice. Therefore, a cheap and environment-friendly approach is significantly important and urgently required for the development of practical high performance Si-based anode.

Herein, novel nanoporous Si/C composites were prepared through spray drying and carbonization method by using NaCl as nanopore template, as shown in Fig. 1a. The simple introduction of NaCl in preparation process, which can be completely removed by routine washing with deionized (DI) water, leads to formation of cubic nanopores in the Si/C composites. Cycle life and rate capability were greatly improved due to the effective accommodation of volume expansion and facilitated Li ions transport.

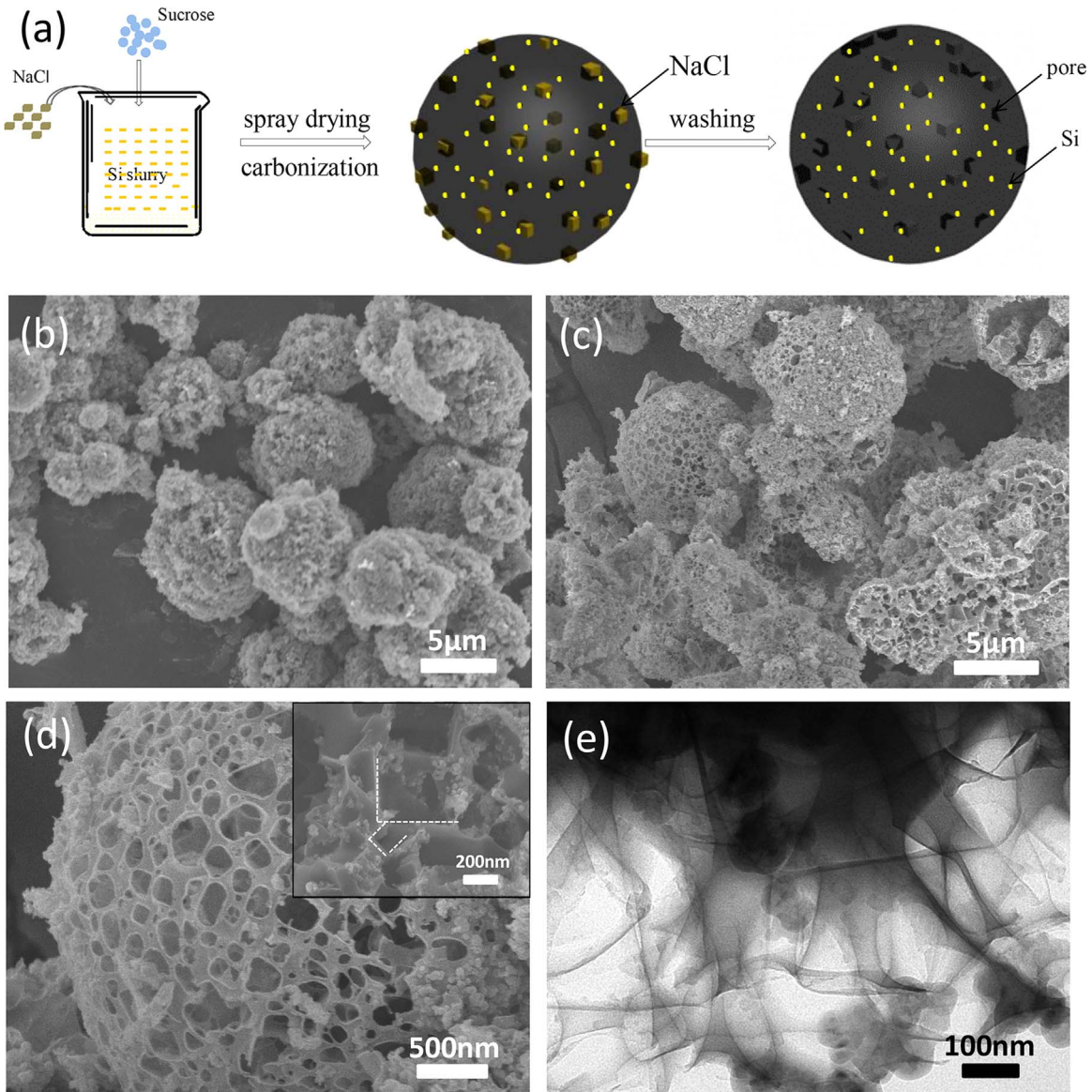
## 2. Experimental

Fig. 1a shows the typical fabrication process of porous Si/C composites. 5 g commercial Si nanoparticles in size of 80–160 nm (Paddy Materials Technology Co., Ltd. Shanghai) were mixed with

---

\* Corresponding authors.

E-mail addresses: [jiangxp64@163.com](mailto:jiangxp64@163.com) (X. Jiang), [wangwei@nimte.ac.cn](mailto:wangwei@nimte.ac.cn) (W. Wang), [liuzp@nimte.ac.cn](mailto:liuzp@nimte.ac.cn) (Z. Liu).



**Fig. 1.** (a) Schematic of fabrication process of porous Si/C composite; (b) SEM image of Si/C-122 before washing; SEM images (c, d) and TEM image (e) of Si/C-122 with different magnifications after washing, inset image in (e) presents the morphology inside Si/C-122.

certain sucrose and NaCl in DI water (See Fig. S1 in Supporting information). After spray drying of the as-prepared mixture, the as-collected powders were heated at 700 °C for 2 h with continuous Ar flow at ambient atmosphere. Then, the Si/C composites were obtained by washing with DI water for three times and drying at 80 °C, which can significantly reduce the Cl contamination to be around 0.01% in the composite. Various samples had been prepared by tuning the weight ratio of Si: sucrose: NaCl. For the precursor ratio of 1:2:2, the sample is named as Si/C-122 for short. The Si/C-121 and Si/C-120 present the samples with precursor ratio of 1:2:1 and 1:2:0, respectively.

The structure characterization of all products was investigated by field emission scanning-electron microscopy (FE-SEM, Hitachi S-4800), transmission electron microscopy (TEM, FEI Tecnai G2 F20), powder X-ray diffraction (XRD) and Thermogravimetric analysis (TG). The nitrogen sorption isotherm (BET) was recorded by a Micromeritics ASAP-2020M nitrogen adsorption apparatus. Pore size distribution plot was obtained by the Barrett-Joyner-Halenda (BJH) method.

The working electrode was prepared by mixing the prepared composites, super P conductive carbon and alginate at a weight

ratio of 80: 10: 10 with DI water as the solvent. The average loading mass densities for all samples are around 1.6 mg/cm<sup>3</sup>. Electrochemical measurements were carried out in CR2032-type coin cells, which were assembled in an argon filled glove box. Diethyl carbonate (DMC) based electrolyte (Zhangjiagang Guotai Huarong Chemical New Material Co., Ltd., S-3215G) and separator (Celgard, 2025) were used. All battery cells were cycled within the voltage window of 0.005–1.5 V by using a battery test system (Jinnuo Wuhan Corp., LANDCT2001A).

### 3. Results and discussion

Fig. 1b shows the SEM image of Si/C-122 composites before washing. As a result of spray drying process, the composites in sharp of sphere with diameter of around 2–10 μm can be obtained. After the routine washing process with DI water, porous structure can be observed as shown in Fig. 1c. With careful observation in high magnification SEM image in Fig. 1d, numerous pores in size of hundreds of nanometers appear on surface. Different from the irregular circular pores formed by sacrificing SiO<sub>2</sub> particles in other

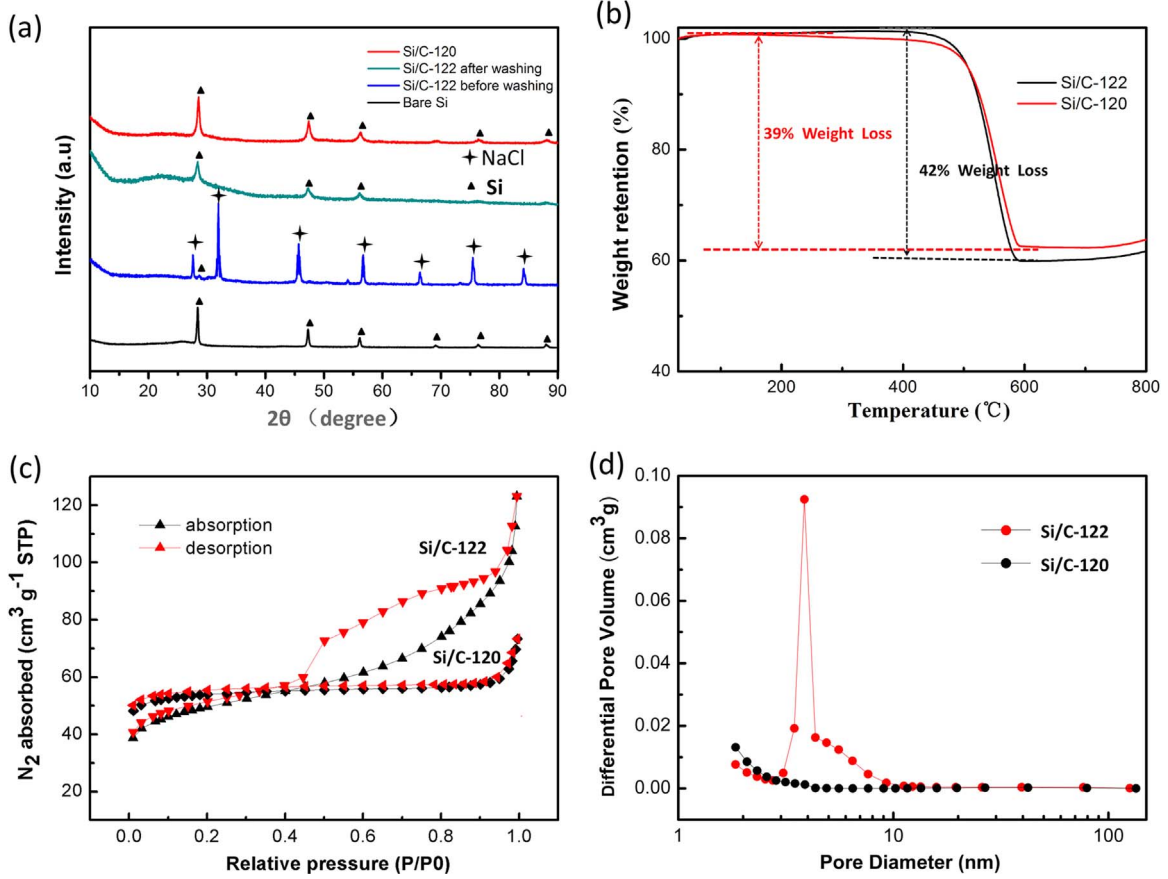


**Fig. 2.** (a) X-ray diffraction patterns of bare Si, Si/C-120, Si/C-122 before and after washing; (b) TG curve of Si/C-120 and Si/C-122; (c) Nitrogen adsorption–desorption isotherm linear plots and (d) pore size distribution of Si/C-122 and Si/C-120 composites.

works [17,18], the pores in this image have clear edges and corners, which might be due to the cubic crystal of NaCl. The sample was also milled for the SEM characterization, as shown in inset image of Fig. 1d, that similar pores also exist inside the Si/C composite. TEM image in Fig. 1e further demonstrates that the pores are in shape of cube with edge length of hundreds of nanometers, which is consisted with the SEM characterization. The Si nanoparticles are randomly distributed in the porous carbon matrix.

Fig. 2a shows XRD patterns of bare Si, Si/C-120 sample and Si/C-122 samples before and after washing process. Both of them have sharp peaks located at 28.4°, 47.3°, 56.1°, 58.8°, 69.1°, and 88.0°, which can be well indexed as the (111), (220), (311), (400), (331) and (422) planes of crystal silicon (JCPDS no. 27-1402). Six additional reflections in the Si/C-122 before washing correspond well with the diffractions of NaCl (JCPDS no. 88-2300). After washing the sample, there is no evidence of NaCl in both Si/C-120 and Si/C-122 after washing. In addition, energy dispersive spectroscopy (EDS) analysis of SC-122 after washing demonstrates that there is no Na and Cl element as seen in Fig. S2 in Supporting information, which confirms that NaCl in composite has been washed away completely. The broad curve at 20–27° suggests the nature of amorphous carbon, which is due to the carbonization of sucrose. TG result in Fig. 2b indicates that there is 58 wt% active Si in Si/C-122 composite and 61 wt% active Si in Si/C-120 composite. To further confirm the internal structural characteristics of these composites, the specific surface area were investigated through the BET N<sub>2</sub> adsorption-desorption isotherms at 77 K, as shown in Fig. 2c and d. The typical type III N<sub>2</sub> adsorption-desorption isotherms of Si/C-122 imply that it composed by macroporous structures. In contrast, the isotherms were not obvious and no

hysteresis loop was observed in Si/C-120. As expected, the BET specific surface areas increase from 67 m<sup>2</sup> g<sup>-1</sup> in Si/C-120–176 m<sup>2</sup> g<sup>-1</sup> in Si/C-122. The pore size distribution exhibits a hierarchical pore structure in Si/C-122 with the peak of mesopores centered at 4 nm. Since the nanopores generated from NaCl crystal is usually as large as 500 nm, no obvious pore peak can be observed below 100 nm. The appearance of mesopores might be triggered by the influence of NaCl crystal on the carbonization.

Fig. 3a compares the electrochemical performance of Si/C composite with or without addition of NaCl in the voltage range of 0.005–1.5 V at 0.2 A/g. For the Si/C-120 without addition of NaCl, the discharge capacity reaches 1294 mAh g<sup>-1</sup> at the initial cycle and then 941 mAh g<sup>-1</sup> at the second cycle. However, it decreases rapidly to less than 400 mAh g<sup>-1</sup> within 50 cycles. After introducing 25 wt% NaCl into the composite Si/C-121, it shows similar discharge capacity of around 900 mAh g<sup>-1</sup> from the second cycles. However, the cycling stability has been significantly improved that the discharge capacity still remains at about 600 mAh g<sup>-1</sup> after 100 cycles. The cycle life can be further enhanced by increasing the content of NaCl to 40 wt% in Si/C-122 sample, which can deliver a high discharge capacity of 1394 mAh g<sup>-1</sup> at the first cycle, 977 mAh g<sup>-1</sup> at the second cycle, 936 mAh g<sup>-1</sup> at the 10th cycle. The total loss in the first 10 cycle is 33%, while the discharge capacity would be stable from the 2nd to 10th cycle with a capacity loss of 3.9%. Finally, the discharge capacity can be remained over 740 mAh g<sup>-1</sup> after 100 cycles with capacity retention of 78%. Here, the tap density of Si/C-122 nanoporous composite was examined to be around 0.59 g/cm<sup>3</sup>, which is much lower than that of the commonly used graphite based anode, such as: MCMB of 1.2–1.5 g/cm<sup>3</sup>. However, it is worth to mention that its

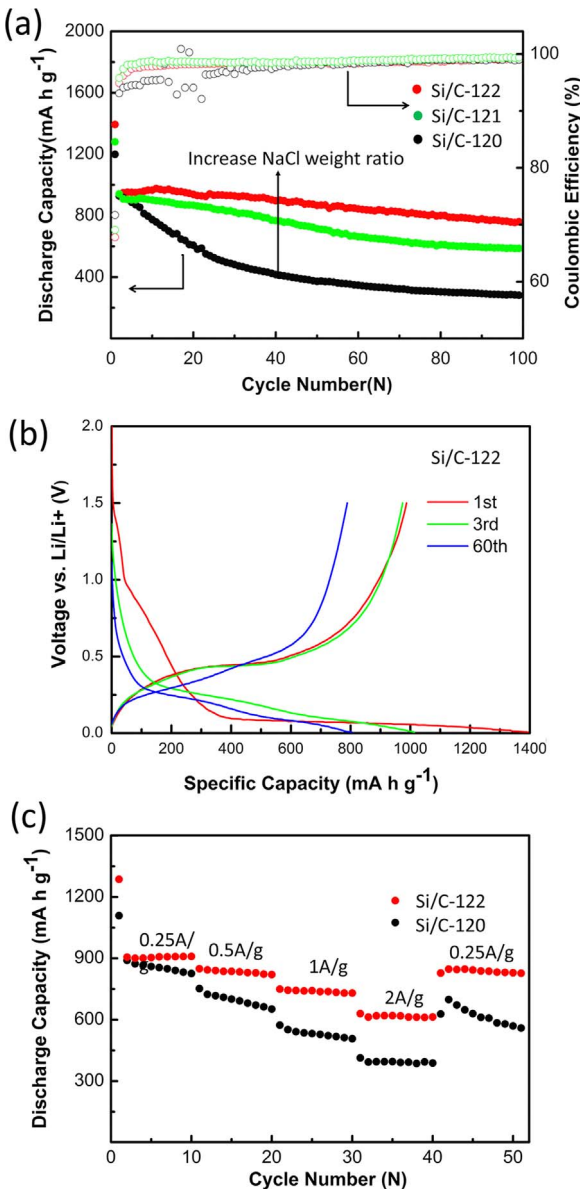


**Fig. 3.** (a) Specific discharge capacities and coulombic efficiencies of Si/C-120, Si/C-121 and Si/C-122 at a current density of  $0.2 \text{ A g}^{-1}$ ; (b) Galvanostatic charge/discharge profiles of the Si/C-122 at the 1st, 3rd and 60th cycle; (c) Rate capabilities of Si/C-122 and Si/C-120.

corresponding gravimetric capacity reaches a stable capacity of  $950 \text{ mAh/g}$  from the 2nd cycle, that is almost three times higher than that of the graphite based anode of  $320 \text{ mAh/g}$ . Thus, the overall volumetric capacity of porous Si/C-122 is still a little higher than that of the graphite based anode, which make it useful in practical battery applications. On the other hand, it is also found that the coulombic efficiency of Si/C-120 is not very stable as the electrochemical test goes, suggesting the unstable structures during the cycling process. Compared to that, the coulombic efficiency of Si/C-122 is higher and more stable, which reaches more than 99% from the 13 cycle. The detailed investigation of electrodes after cycling demonstrates that the nanopores help a lot to maintain the structure stability during electrochemical cycling, as shown in Fig S3 in Supporting information. Fig. 3b shows the corresponding voltage vs. capacity plot of Si/C-122 electrode at the 1st 3rd and 60th cycle. It can be clearly seen that the first charge (lithiation) and discharge (delithiation) capacities are  $1394 \text{ mAh g}^{-1}$  and  $957 \text{ mAh g}^{-1}$ , respectively. The corresponding

coulombic efficiency (CE) is 68.7%, which is might be due to the irreversible transition from crystalline Si to amorphous  $\text{Li}_x\text{Si}$ , the formation of irreversible solid electrolyte interphase (SEI) layer and large BET surface area [5]. Moreover, the rate capability of Si/C composite can also be improved by the addition of NaCl. Fig. 3c shows the rate performance of Si/C-120 and Si/C-122 at current density of  $0.25 \text{ A g}^{-1}$ ,  $0.5 \text{ A g}^{-1}$ ,  $1 \text{ A g}^{-1}$  and  $2 \text{ A g}^{-1}$ , respectively. After doubling the current density every ten cycles, the discharge capacities of Si/C-120 are  $889 \text{ mA h g}^{-1}$ ,  $724 \text{ mA h g}^{-1}$ ,  $551.4 \text{ mA h g}^{-1}$ ,  $392 \text{ mA h g}^{-1}$ . At the high current density of  $2 \text{ A g}^{-1}$ , the discharge capacity is as low as  $392 \text{ mA h g}^{-1}$  that is only less than half of the initial capacity at current density of  $0.25 \text{ A g}^{-1}$ . In contrast, the Si/C-122 reveals a much better rate performance. The discharge capacities can reach  $905 \text{ mA h g}^{-1}$ ,  $843 \text{ mA h g}^{-1}$ ,  $744 \text{ mA h g}^{-1}$  and  $613 \text{ mA h g}^{-1}$  at the current density of  $0.25 \text{ A g}^{-1}$ ,  $0.5 \text{ A g}^{-1}$ ,  $1 \text{ A g}^{-1}$  and  $2 \text{ A g}^{-1}$ , respectively. A much higher discharge capacity of  $613 \text{ mA h g}^{-1}$  can be achieved at the high current density of  $2 \text{ A g}^{-1}$ . Moreover, the discharge capacity of Si/C-122 can be recovered to similar level when the current density is set back to  $0.25 \text{ A g}^{-1}$ , compared to the obvious loss in Si/C-120. This result strongly demonstrates that the generation of nanopores by introduction of NaCl does improve the kinetics processes of lithiation/delithiation.

#### 4. Conclusion

Nanoporous Si/C composites were successfully fabricated through a spray-drying and carbonization process with the help of environmentally benign NaCl as sacrificing template. The formation of cubic nanopores in Si/C composite plays the significant role in improving the cycle and rate capability. A high discharge capacity of around  $900 \text{ mA h g}^{-1}$  can be achieved with capacity retention of 78% after 100 cycles. This method is simple and versatile for fabricating nanoporous structure in an environment-friendly way, and thus is suitable for various energy storage applications in practice.

#### Acknowledgement

This work is supported by the National Natural Science Foundation of China (51402322) and the Natural Science Foundation of Zhejiang (LY13A040005).

#### Appendix A. Supplementary material

Supplementary data associated with this article can be found in the online version at <http://dx.doi.org/10.1016/j.matlet.2016.05.092>.

#### References

- [1] J.M. Tarascon, M. Armand, Issues and challenges facing rechargeable lithium batteries, *Nature* 414 (2001) 359–367.
- [2] M.R. Zamfir, H.T. Nguyen, E. Moyen, Y.H. Lee, D. Pribat, Silicon nanowires for Li-based battery anodes: a review, *J. Mater. Chem. A* 1 (2013) 9566.
- [3] N. Liu, Z.D. Lu, J. Zhao, M.T. McDowell, H.W. Lee, W.T. Zhao, et al., A pomegranate-inspired nanoscale design for large-volume-change lithium battery anodes, *Nat. Nanotechnol.* 9 (2014) 187–192.
- [4] J.W. Kim, J.H. Ryu, K.T. Lee, S.M. Oh, Improvement of silicon powder negative electrodes by copper electroless deposition for lithium secondary batteries, *J. Power Sources* 147 (2005) 227–233.
- [5] Q.Z. Xiao, Y. Fan, X.H. Wang, R.A. Susantyoko, Q. Zhang, A multilayer Si/CNT coaxial nanofiber LIB anode with a high areal capacity, *Energy Environ. Sci.* 7 (2014) 655–661.

- capacity-limited cycling, *J. Power Sources* 205 (2012) 433–438.
- [6] Y.Q. Zhang, X.H. Xia, X.L. Wang, Y.J. Mai, S.J. Shi, Y.Y. Tang, et al., Three-dimensional porous nano-Ni supported silicon composite film for high-performance lithium-ion batteries, *J. Power Sources* 213 (2012) 106–111.
  - [7] M.S. Park, Y.J. Lee, S. Rajendran, M.S. Song, H.S. Kim, J.Y. Lee, Electrochemical properties of Si/Ni alloy-graphite composite as an anode material for Li-ion batteries, *Electrochim. Acta* 50 (2005) 5561–5567.
  - [8] L.F. Cui, R. Ruffo, C.K. Chan, H.L. Peng, Y. Cui, Crystalline-Amorphous Core-Shell Silicon Nanowires for High Capacity and High Current Battery Electrodes, *Nano Lett.* 9 (2009) 491–495.
  - [9] Y. Yao, M.T. McDowell, I. Ryu, H. Wu, N. Liu, L. Hu, et al., Interconnected silicon hollow nanospheres for lithium-ion battery anodes with long cycle life, *Nano Lett.* 11 (2011) 2949–2954.
  - [10] H. Ma, F. Cheng, J.Y. Chen, J.Z. Zhao, C.S. Li, Z.L. Tao, et al., Nest-like silicon nanospheres for high-capacity lithium storage, *Adv. Mater.* 19 (2007) 4067–4070.
  - [11] S. Ohara, J. Suzuki, K. Sekine, T. Takamura, A thin film silicon anode for Li-ion batteries having a very large specific capacity and long cycle life, *J. Power Sources* 136 (2004) 303–306.
  - [12] X. Huang, J. Yang, S. Mao, J. Chang, P.B. Hallac, C.R. Fell, et al., Controllable synthesis of hollow Si anode for long-cycle-life lithium-ion batteries, *Adv. Mater.* 26 (2014) 4326–4332.
  - [13] J. Cho, Porous Si anode materials for lithium rechargeable batteries, *J. Mater. Chem.* 20 (2010) 4009.
  - [14] L. Su, Z. Zhou, M. Ren, Core double-shell Si@SiO<sub>2</sub>@C nanocomposites as anode materials for Li-ion batteries, *Chem. Commun.* 46 (2010) 2590–2592.
  - [15] J.B. Park, K.H. Lee, Y.J. Jeon, S.H. Lim, S.M. Lee, Si/C composite lithium-ion battery anodes synthesized using silicon nanoparticles from porous silicon, *Electrochim. Acta* 133 (2014) 73–81.
  - [16] H. Wu, G.Y. Zheng, N.A. Liu, T.J. Carney, Y. Yang, Y. Cui, Engineering Empty Space between Si Nanoparticles for Lithium-Ion Battery Anodes, *Nano Lett.* 12 (2012) 904–909.
  - [17] Z. Li, W. Wang, Z. Li, Z. Qin, J. Wang, Z. Liu, Bridging porous Si-C composites with conducting agents for improving battery cycle life, *J. Power Sources* 286 (2015) 534–539.
  - [18] Q.J. He, C.H. Xu, J.Q. Luo, W. Wu, J.L. Shi, A novel mesoporous carbon@silicon-silica nanostructure for high-performance Li-ion battery anodes, *Chem. Commun.* 50 (2014) 13944–13947.